Received: 17 January 2022 | Revised: 23 May 2022 | Accepted: 12 July 2022

DOI: 10.1002/hyp.14658

RESEARCH ARTICLE

WILEY

Measuring zero water level in stream reaches: A comparison of an image-based versus a conventional method

Amelie Herzog[1] | Kerstin Stahl[1] | Veit Blauhut[1] | Markus Weiler[2]

[1]Chair of Environmental Hydrological Systems, University of Freiburg, Baden-Württemberg, Germany

[2]Chair of Hydrology, University of Freiburg, Baden-Württemberg, Germany

Correspondence
Amelie Herzog, Chair of Environmental Hydrological Systems, University of Freiburg, Freiburg im Breisgau, Baden-Württemberg 79098, Germany.
Email: amelie.herzog@hydrology.uni-freiburg.de

Funding information
Badenova Fund For Innovation

Abstract

A limited number of gauging stations, especially for nested catchments, hampers a process understanding of the interaction between streamflow, groundwater and water usage during drought. Non-commercial measurement devices can help overcome this lack of monitoring, but they need to be thoroughly tested. The Dreisam River in the South-West of Germany was affected by several hydrological drought events from 2015 to 2020 during which parts of the main stream and tributaries fell dry. Therefore it provided a useful case study area for a flexible longitudinal water quality and quantity monitoring network. Among other measurements the setup employs an image-based method with QR codes as fiducial marker. In order to assess under which conditions the QR-code based water level loggers (WLL) deliver data according to scientific standards, we compared its performance to conventional capacitive based WLL. The results from 20 monitoring stations reveal that the riverbed was dry for >50% at several locations and even for >70% at most severely affected locations during July and August 2020, with the north western parts of the catchment being especially concerned. Highly variable longitudinal drying patterns of the stream reaches emerged from the monitoring. The image-based method was found valuable for identification and validation of zero level occurrences. Nevertheless, a simple image processing approach (based on an automatic thresholding algorithm) did not compensate for errors due to natural conditions and technical setup. Our findings highlight that the complexity of measurement environments is a major challenge when working with image-based methods.

KEYWORDS
hydrological drought, innovative sensors, longitudinal connectivity, stream reaches, streamflow intermittency, zero flow

1 | INTRODUCTION

Periodic and temporary streamflow may occur naturally in Intermittent Rivers and Ephemeral Streams (IRES; Leigh & Datry, 2017; Datry et al., 2017). The proportion of IRES in the global river network is estimated at 30% excluding and 50% including headwater streams (Costigan et al., 2016; Fortesa et al., 2021). Regime shifts from perennial to intermittent streamflow are estimated to occur more often in the future, also on the Northern Hemisphere (Döll & Müller Schmied, 2012) and could have severe consequences for riverine

ecosystems, especially where aquatic biota is not adapted to temporary drying (Acuña et al., 2020; Leigh & Datry, 2017). In addition, the most extreme form of low flows is a partial or full drying-up of streambeds and such hydrological droughts have exacerbated in many regions (van Loon, 2015). Therefore, monitoring and understanding the dynamics of IRES has been given rising attention in recent research.

Activation and deactivation patterns of river networks and can also be described using statistical or hierarchical models (Botter et al., 2021; Botter & Durighetto, 2020; Durighetto et al., 2020; Godsey & Kirchner, 2014; Lovill et al., 2018; Senatore et al., 2021). While these approaches allow mapping and modelling of the active streamlength and drainage density, they are not primarily concerned with processes along rivers and ecological implications of IRES. For research about interdisciplinary impacts, the concept of aquatic states has therefore evolved and is widely used for classification of IRES (Fovet et al., 2021; Leigh & Datry, 2017; Meerveld et al., 2020; Messager et al., 2021; Pastor et al., 2022). The concept defines three hydrological phases (flowing, standing, dry) corresponding to the different habitats (lotic, lentic, terrestial) generated in response to different flow conditions (Costigan et al., 2016; Datry et al., 2017; Gallart et al., 2017).

Up to date, classification of the hydrological regimes of IRES is hindered by a lack of continuous observations and status data (water, no water, flow, no flow). In global hydrometric datasets, stream reaches and streams with a mean annual flow $< 50\,m^3s^{-1}$ are likely to be underrepresented (Messager et al., 2021). Due to this data gap, simulating and predicting streamflow intermittency has often been based on spatial predictors, such as topography, slopes or drainage area, transmissivity (Kaplan et al., 2019; Olson & Brouillette, 2006) and has often been validated using hydrographic maps or field mapping (e.g., Botter & Durighetto, 2020; Durighetto et al., 2020; Jensen et al., 2017; Jensen et al., 2018; Shaw et al., 2017; Ward et al., 2018; Zimmer & McGlynn, 2017).

In practice, many gauging stations make use of water level data and calculate streamflow at any given time based on rating curves and streamflow field measurements. However, water level information remains an at-site point information taken at one isolated cross-section of the stream. Moreover, zero flow and zero water level measurement is challenging to gauge with conventional techniques because installation errors of measurement devices, data errors and ambiguity hinder a correct interpretation of zero flow readings (Heiner et al., 2011; Zimmer et al., 2020). The heterogeneity of the stream bed due to changing flow conditions and sediment transport may lead to erroneous identification of zero flow or zero water level, for example if ponding occurs locally along the river section. If occurrence of zero-flow or zero-water level is not measured with sufficient accuracy and temporal and spatial resolution, also models for water resource management and for the prediction of drought and low flows will remain uncertain as they require reliable data of these states for validation and calibration (Hannah et al., 2011).

The development of non-conventional sensors for in situ monitoring has become useful to gather more observational data on stream reaches. The simplicity of the installation in remote areas, the potential to measure continuously with high resolution, the affordable cost and therefore less risk of financial losses in case of damages, and other advantages make them an attractive alternative to conventional methods (Chapin et al., 2014). In particular, electrical conductivity and temperature loggers (Bhamjee et al., 2016; Blasch et al., 2002; Larson & Runyan, 2009; Peirce & Lindsay, 2015; Zanetti et al., 2022; Zimmer & McGlynn, 2017) and float switch or flow sensors (Assendelft & van Meerveld, 2019) have been successfully used to monitor aquatic state changes of small headwater streams and stream reaches. To study the connectivity of stream networks for ungauged catchments and areas suffering from data scarcity the use of remote sensing is often proposed (Gleason & Smith, 2014; Stoll & Weiler, 2010). Disadvantages of the latter are however the low temporal resolution and data gaps due to obstacles such as cloud cover (Spence & Mengistu, 2016). In general, aerial surveys are not applicable in areas with dense tree cover along streams (Roelens et al., 2018) and vegetation's moisture may lead to misinterpretation (Eltner et al., 2018; Spence & Mengistu, 2016). On-site image-based techniques are increasingly applied for monitoring. They contain an additional visual information that reduced the probability of misinterpretation (Leduc et al., 2018). An advantage is that they do not require on-site calibration (Gilmore et al., 2013; Kaplan et al., 2019; Leduc et al., 2018; Young et al., 2015), for example, detected the edge position of streams manually and assumed that each edge coordinate is linearly related to the water stage. They used a width-stage relationship to derive streamflow. Particle image velocimetry (PIV) also belongs to this group of methods but water velocity is measured directly using short videos (Perks et al., 2020; Piton et al., 2018). Another option to obtain information on the water level or streamflow is to use image pattern recognition algorithms (Elias et al., 2020; Eltner et al., 2018; Eltner et al., 2021), staff gauges (Bruinink et al., 2015; Seibert et al., 2019; Strobl et al., 2020; Zhang et al., 2019) or fiducial grid patterns (Gilmore et al., 2013; Kaplan et al., 2020). The quality and resolution of the data obtained with image-based methods is still lower in comparison to traditional gauging methods. But the significantly lower cost and the simplicity of the method allows a broader application (Eltner et al., 2018; Royem et al., 2012; Schoener, 2018). Applications for citizen science and crowd-based water level measurements also makes use of image-based methods (Etter et al., 2020; Strobl et al., 2020; Seibert et al., 2019). The risk of errors due to measurement installation and maintenance is lower but the information is not collected during fixed time intervals and the content may deviate depending on the person who collected the data. The use of fiducial markers in citizen science is promising because it transports an exact value when recognized correctly.

The catchment of the Dreisam river in south western Germany is known as a perennial river; But its tributaries as well as parts of the upper and lower main stream can fall dry during extreme meteorological drought events, such as in the years 2003 and 2018 (Erfurt et al., 2020). During such hydrological drought situations, the main gauging station, located in the Dreisam Valley at Ebnet upstream of

Freiburg, has been found not to be representative of the severity of water level and flow conditions across the basin (Blauthut et al., 2017). Until a recent reconstruction of the station's crosssection (HVZ-Baden-Württemberg, 2021), zero water levels could not be derived from the multiple decades-long time series of hydrometric data from the main gauging station in the valley due to uncertainties for recordings of water levels below 20 cm. In addition, hydrological dynamics of different river reaches might be different in comparison to the location of the gauging station depending on the hydraulic properties and the geometry of the riverbed and its interaction with the groundwater. Hence, the main gauging station has provided little indication of the true dry river conditions in the valley. To better understand the drying pattern in the catchment a network of water level gauges was installed. It allowed to monitor a hydrological drought event in 2020 with three governing questions:

1. Is it possible to use an image based method for water level measurements based on QR-code detection?
2. What are problems and possible causes related to a QR-code image based water level logging?
3. Is it possible to identify zero level occurrences and drying patterns of the stream reaches using the specific measurement techniques?

To answer these questions, we compare the time series of two different measurement methods: an image-based measurement method using QR-codes as fiducial markers and a conventional capacitive Water Level Loggers (WLL) technique. We explore the range, temporal evolution and the correlation of the water level time series measured with both methods at 11 locations in the study area. Subsequently, we identify potential error sources for the measurement of zero water levels using image-based WLL and propose specific corrections for different error sources. We then implement a method to determine zero water level occurrences and use the image-based method as an additional source of information to validate the event selection. The obtained drying patterns enable an analysis of longitudinal connectivity in the catchment.

2 | METHODS

2.1 | Measurement approach

The water level (often also refered to as river stage, water height, stage height) is described as the perpendicular distance from the bottom of the riverbed to the water surface. An advantage of image-based measurements is that the additional visual information contained in each image provides an additional possibility to validate the dry status of the riverbed (Gilmore et al., 2013; Kaplan et al., 2019; Royem et al., 2012; Schoener, 2018; Zhang et al., 2019). In order to obtain an information on the water level, a reference point or fiducial marker is necessary. The three position markers implemented in the structure of QR-Codes allows the recognition of the marker in images independent of their location on the actual image (Pandya & Galiyawala, 2014). Using QR-Codes as a fiducial marker thus does neither require the detection of a water line on the image, nor does it require the definition of a region of interest as it is often required image-based water level measurement (Chapman et al., 2020; Eltner et al., 2021; Kuo & Tai, 2022; Young et al., 2015; Zhang et al., 2019). Another advantage of QR-codes is that they are still readable if part of them are not well visible. Due to numerous industrial applications, a selection of open source libraries (Abeles, 2013; Abeles, 2016; Hudson et al., 2015) is available for the detection of QR-codes, which faciliates the implementation of QR-Codes as fiducial marker for the measurement of water levels. In our measurement setup QR-codes (Figure 1) were printed onto a HPL (high pressure laminat) panel (dimensions 60x85cm). Each QR-Code covers 10x10cm. The horizontal distance between the codes is 44 mm and the vertical distance is 20 mm. Between the columns, there is a vertical offset of 33 mm. A key factor for the choice of the size and placement of the QR-codes (in order to guarantee recognition) is to find the optimal compromise between picture resolution and the distance between the camera and the panel. In our setup, each QR-code represents a distinct water level of $0-72$cm in steps of 3 (a total of 25 QR-codes per panel; Figure 1, Table 1). With this QR-code configuration, the water level can thus be measured at a maximum accuracy of 3cm. The lowest QR-Code recognized by the software is representative for the water level. The camera used is a DOERR SnapShot Mini 5.0 wildlife camera and measures at an image resolution of 8 MP. During nighttime, the camera automatically switches to infrared mode while lowering the resolution. The cameras take an image every 15 min. This high temporal resolution was chosen to capture fast water level rise and recession. A battery with an initial electric potential of 6.5 V and an electric charge of 4.5 Ah was used.

A variety of software solutions to read QR-codes due to the numerous applications of QR-codes in industry and other sectors are available (reviewed by Abeles, 2018). For our study, the QR-codes are read using the python wrapper pyboof for the java library BoofCV (Abeles, 2016, 2021). The approach detects the positioning detection markers of a QR code and the alignment markings. According to a performance evaluation of the provider, BoofCV is able to read multiple QR codes in one image, while the processing time is not longer than with other packages. For all of the available QR code software, damaged QR codes, images with bright spots and non-compliant QR codes are problematic for detection performance of the software. The package was also chosen because it can be implemented on a Rasperry PI (Linux-based single-board computer) allowing automatic data transmission in the future. Additionally, an android app is already available for BoofCV for easy handling or citizen science advancement.

The second method used in this study is a capacitive water level observation. An Odyssey Capacitance water level logger (Ody Ltd, 2013) was installed at every measurement location. It measures the capacity of a condensator consisting of a teflon coated wire and the water in the river bed. Teflon coating is the dielectric between the wire and the water. The higher the water level, the larger is the plate of the condensator and thus, the higher the measured voltage. The Ody loggers can measure with an accuracy of ± 0.5cm (Table 1). Each

FIGURE 1 Measurement setup Wagensteig tributary summer 2020

logger was calibrated in a laboratory environment. Ody loggers were installed in the field using PVC pipes (Figure 1). Considering the technical properties of both measurement methods alone, QR has a lower accuracy and requires also more effort for post processing (Table 1).

2.2 | Image processing

Errors due to image-based water level measurements can be classified into three categories according to (Gilmore et al., 2013): Errors due to the quality of the pictures also mentioned in (Leduc et al., 2018), due to local environment (light conditions) or due to software and image recognition. To reduce the effect of the errors on the final data set, processing techniques can be used to select erroneous images before (pre-processing) or to select erroneous values after the actual QR code recognition (post-processing). The software deals with some of these error types. In the case of images with over exposure and strong light reflections, the software will not recognize a QR code and ultimately issue a NAN value. Erroneous values can then be excluded. However, pre-processing might be valuable in order to reduce the number of images to be read and hence the total computational effort and time needed for conversion of the image data set into a time series of water levels (although this also depends on the computer system used). Images with overexposure and strong light reflections can be filtered using a threshold on the grey-scale image for bright colours. Major inaccuracies in the water level data set however, are caused by images with few light reflections and with sediment accumulation. In such cases, the information on a single QR code is lost where light reflections or sediment accumulation occur but the software still reads the remaining QR codes. Sediment accumulations occur most likely on the bottom of the QR code panel below the water surface and deposits remain on the panel once the water level decreases. The derived water level will thus be biased towards higher values in comparison to the actual, true water level. This may also be

TABLE 1 Main properties of the measurement methods

	Image-based WLL	Capacitive WLL
Method	QR	Ody
Data transmission	manual	manual
Accuracy	3 cm	±0.5 cm
Data processing	Yes	No
Pre-/post-processing	Yes	No

Abbreviation: WLL, water level loggers.

the case for images with few light reflections, if those appear on the bottom of the visible part of the QR code panel right above the water surface.

In this study, we chose benchmark images with sediment accumulation, strong light reflections, relatively few light reflections and overexposure (Figure 2) to investigate if it is possible to filter images with theses issues (Table 2) by means of a multi-threshold approach. Hereby, multiple thresholds are defined based on the intensity of grey scale values of the pixels in an image. The thresholds can either be specified manually or using an algorithm for automatic thresholding. Due to their accuracy and speed, algorithms that are calculating thresholds by maximization of between-class variance (Otsu's method) are commonly used (Kotte et al., 2018; Otsu, 1979). We use a Multi Otsu threshold with 5 classes (0–4). Thus, the different pixels can be classified into different 'regions' based on these thresholds (Figure 2). Region 0 contains pixels of lowest intensity (black) while region four contains pixels of highest intensity (white). Ideally, the pixels concerned by one of the error sources belong to one specific region. If the number of pixels in an image belonging to this specific region is large in comparison to the number of pixels in this region in an image with normal conditions, the image is most likely affected by the error source and can be removed; for example, for strong light reflections, the amount of pixels with very high intensity is expected to be larger with respect to an image with normal light conditions.

To identify overexposure and light reflections, the percentage of pixels in region 4 with respect to total pixels ($P_{pix}(4)$) and to identify sediment accumulation, the percentage of pixels in region 3 with respect to total pixels ($P_{pix}(3)$) was calculated using Equation (1). $Np(region)$ is the number of pixels for the specific region and Np_{tot} is the total number of pixels of the image.

$$P_{pix}(region) = \frac{Np(region)}{Np_{tot}} \cdot 100 \quad (1)$$

Using this approach, it is possible to distinguish between strong overexposure or strong light reflections and normal conditions (Table 2). However, it is challenging to distinguish between normal conditions and sediment accumulation or few local light reflections in the image. The filtering of such images is complex and therefore, a specific methodological approach needs to be applied rather than a simple algorithm for automatic thresholding.

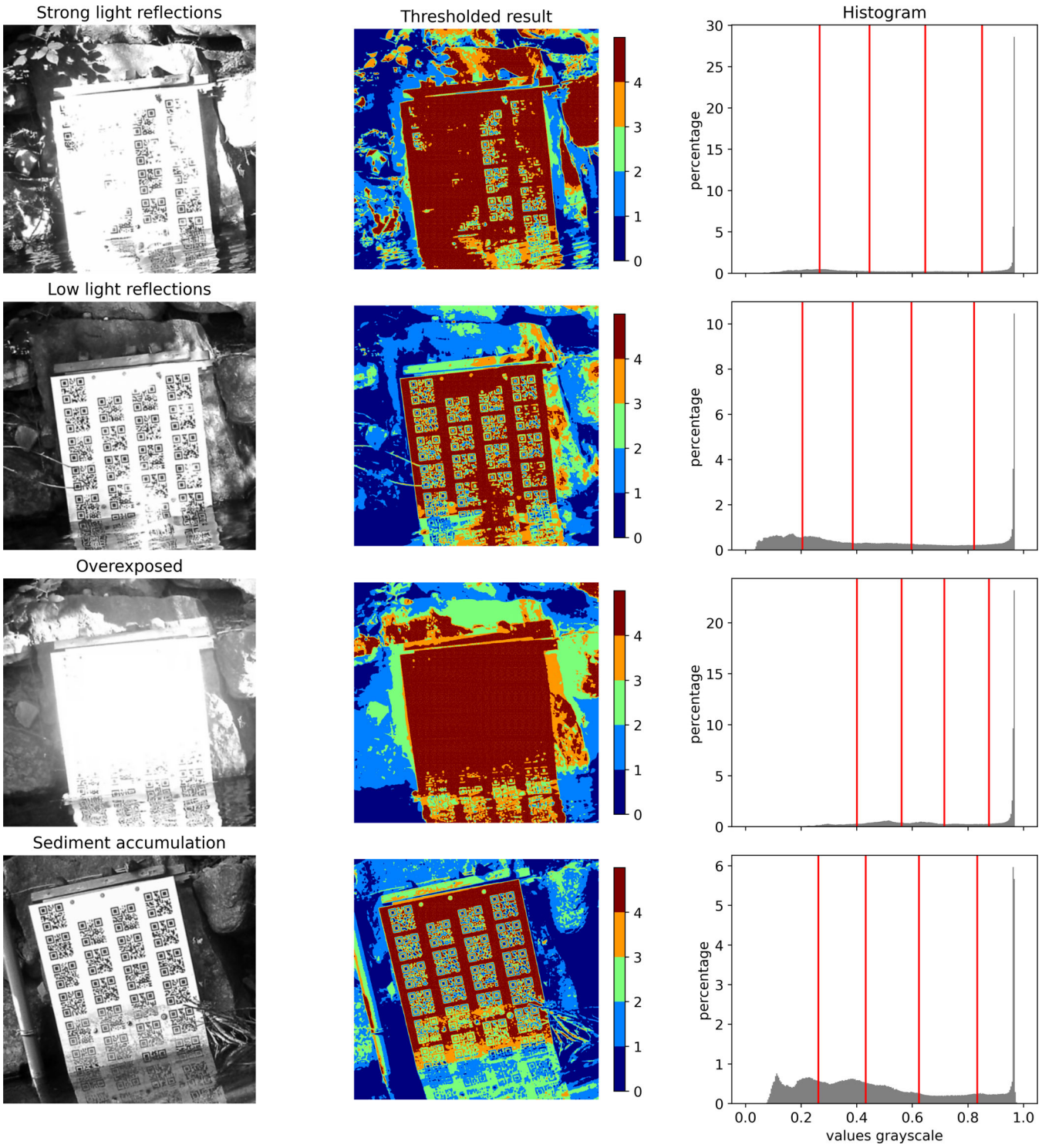

FIGURE 2 The benchmark images for the different error sources, histograms with thresholds depicted by vertical red lines and the resulting classification after Multi-Otsu thresholding with the pixels coloured per region they belong to

Due to the complexity of filtering the QR code images and the lower accuracy in comparison to the Ody measurements (which would call for an entire study of its own), we used only the Ody data for data analysis and selection of zero level occurrences. However, we can make use of the visual information in the images in order to validate the zero level occurrences based on the Ody data.

2.3 | Zero water level definition

Zero water level means that there is no more water present at the deepest point of the river cross section and that there is neither flowing nor standing water present in the riverbed. To retrieve the IRES status information (dry, standing water, flowing water), a distinction

TABLE 2 Counted pixels per region

Benchmark image	Region	P_pix (%)	Error type
Normal	3	12.01	Deposits
Sediment accumulation	3	11.38	
Normal	4	20.27	Light conditions
Light reflections	4	16.01	
Strong reflections	4	44.84	
Overexposure	4	44.88	

has to be made between zero water level and zero flow conditions (Datry et al., 2017; Meerveld et al., 2020). The methods presented in this study only focus on the distinction between the dry and the wet status. The determination of the status change from flowing to standing water could either be achieved manually through visual inspection of the images or through the development of an algorithm (e.g., using neural networks) for recognition of flow patterns. Both was not within the scope of this work but could potentially be implemented in the future. Another limitation of the method is, that the water level is only measured directly at one specific spot due to the installation of the measurement devices at one specific point along the river at the border of the river bed next to the river bank. Ponding can not be directly measured if the measurement device is not located at the deepest point in the river bed section, a point which may change after each sediment transport event.

If there is a vertical offset between the deepest point of the river bed and the location of the measurement device, it is difficult to distinguish if the riverbed is entirely dry or if it is only dry at the borders while standing water remains at the deepest point. To make a distinction here, the water level, at which the water is likely standing and not flowing anymore needs to be known. However, the point of no flow is site specific as it depends largely on the hydraulic properties and geometry of the river section (and not only on the cross-section of the river bed) and therefore, the generation of a rating curve for each location is a prerequisite. This should be kept in mind if any of the presented methods are used to establish a data-set of zero water levels.

Potential sources of inaccuracy for both measurement methods can be due to measurement installation and measurement principle. Specifically for the QR method, a software is required to read the images in order to obtain an information from the fiducial markers on the images. The result of the measurement thus also depends largely on the quality of the image, the local environment (light conditions) and on the software and image recognition algorithms used (Gilmore et al., 2013). The quality of the image and the chances for recognition of the fiducial marker also rely on the ratio of the distance of the panel and the camera and on the focal point.

In order to measure zero water level with the measurement methods used in this study, corrections are required for both, the capacitive and the image based method. Corrections of the QR data can be needed (1) for specific locations where the panel position is not vertical and (2) where there is an offset between the bottom edge of the panel and the bottom of the river bed. However, specific care was taken in order to avoid inclination and a vertical offset of the QR panels and accordingly no offset correction was required for the QR data. An offset correction was however necessary for the Ody data. The Ody loggers are hanging vertically in PVC tubes without direct connection to the bottom of the river bed. Also, water levels measured by the Ody loggers may overestimate water levels for low electrical conductivities due to remaining soil moisture once the riverbed is already dry. A small, positive offset of the Ody measurements is therefore expected. To take both of these possible offsets into account, we applied a correction based on the minimum in the time series. This means that a low water level between 0 and 10 cm is measured once the water level reaches zero. A correction of this offset can either be done manually using the pictures from the cameras installed at most of the stations or by defining an offset. Here, the the offset was corrected by the mean of the minima in the Ody water level time series for all stations, where a minimum value below 10 cm had been measured.

2.4 | Measurement comparison

The main objective of this study is the assessment of different error sources of the image-based and a capacitive water level logging with regard to measurement of zero water level. For this purpose, we assumed that a correction using the deepest point in the river bed cross section is not required. In a first step, we compare the performance of the measurement methods with regard to data availability, time and effort for maintenance as well as for the evaluation and data handling. Furthermore, we compared the water levels measured with both methods.

A general measure to investigate the strength and direction of an association between two variables is the correlation coefficient *r*. Here, we calculated the Spearman rank correlation for a rolling window with a window width of 96 steps (equals 1 day). This allows to evaluate whether the water levels are rising or falling at the same moment or not within the time interval of a day and if this association changes over the course of time. Subsequent to the method comparison and the corrections, a method for filtering of zero level occurrences from the available time series is presented. Zero level occurrences were selected based on the choice of a threshold and the coefficient of variation. First, the *t* was defined as the sum of the minimum and 5% of the maximum value in the time series:

$$T = x_{min} + 0.05x_{max} \quad (2)$$

with x_{min} and x_{max} being the minimum and maximum in the time series at each measurement location. In a next step, the coefficient of variation (CV) based on a hourly mean (or daily mean) was calculated. If the CV remained below 0.1 with respect to the hourly mean for at least 4 h at a specific time, it was considered that zero water level occurred. The 4 h hereby represent a generalized time threshold for our specific study catchment. The best suitable time threshold may vary depending on the measurement environment (see also section 5.3).

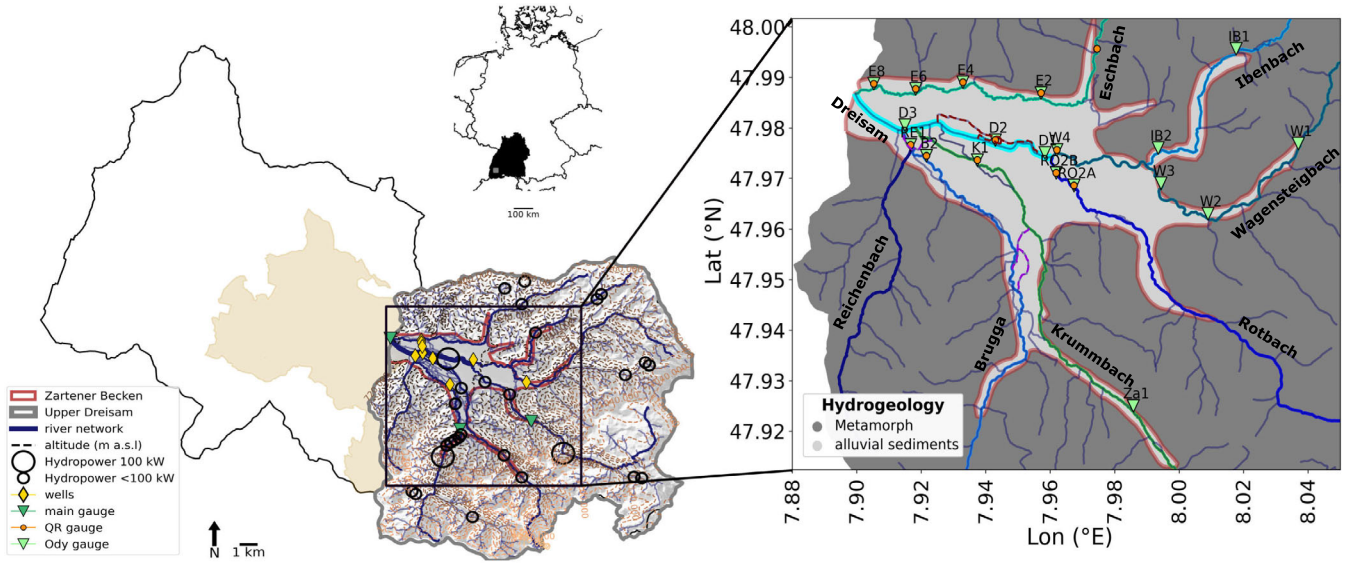

FIGURE 3 Overview of the extent of the Dreisam catchment in South Western Germany, the upper part of the Dreisam catchment and the monitoring system in the Dreisam valley (25 km²)

Furthermore, the additional visual information contained in the QR images allows a validation of zero level occurrences for each location. Images corresponding to the date and time of the zero level occurrences were selected to check for false positive errors. All other images were used to check for false negative errors, i.e. those for which no zero level was found in the Ody time series. Due to the time lag between Ody and QR measurements, it can be assumed that zero level occurrences start earlier (when soil moisture is still high) and end later (when soil moisture increases) than measured with the Ody method. Images 1 day before zero level started and 1 day after zero level ended were therefore excluded from the selection for the validation exercise. The selected images were then visually inspected and classified as 'dry' and 'not dry'. Hereby, a dry riverbed corresponds to the status where there is neither standing nor flowing water visible in the image. Finally, the percentage of images (among a random choice of 10% of all images) recognized as 'dry' (false positives) or 'not dry' (false negatives) defined if the validation was successful or not.

3 | THE STUDY AREA

The Dreisam catchment covers a total area of 577 km^2. Figure 3 shows the catchment and the locations of the measurement devices in the Dreisam valley (25 km^2). The length of the river network in the Dreisam valley is about 108 km. The average streamflow measured at the main gauging station in Ebnet is 5.7 $m^3 s^{-1}$ (HVZ-Baden-W rttemberg, 2021). The porous aquifer consists of alluvial materials with 30 – 50m depth and it is used as a main source of water supply of the city of Freiburg im Breisgau. Within the Dreisam valley, terrains is flat and slopes are gentle (8%), while hillslopes on the edges are steep transitions to the mountainous higher-elevation parts of the catchment. Elevation ranges between 309 m a.s.l. at the lowest point and 1480 m a.s.l. at the highest point (Feldberg) of the catchment (Wissmeier & Uhlenbrook, 2007). The area around the Feldberg summit in the Black Forest upstream of the Dreisam valley (Feldberg area) has a mean snow cover extent of about 37% between October and April (Sauter et al., 2010) and snow is an important contribution to streamflow in spring.

The monitoring system in the Dreisam valley consists of 20 measurement stations located in the main tributaries and the main river (Dreisam; Figure 3). At 11 locations, the water level is measured with both, the QR and Ody method. The maximum and the minimum distance of the measurement locations from the catchment outlet in Ebnet is 13.4 km (W1) and 0.5 km (E8). Riverbed width of the tributaries ranged between 2 m for smaller and 8 m for wider stream reaches in October 2020 (widths around 10 were only measured in the Dreisam itself), though it varies according to flow conditions. The length of the single tributaries varies between 8 and 19 km and the subcatchment areas between 13 and 47 m^2 (see Table 1 in Data S1). Drying events from observations and reporting by public media in specific river sections during the previous years guided the initial choice of the location.The selection of measurement locations generally aimed to gauge regular distances to the mouth of the tributary into the main river. Measurements should represent a longitudinal section of the stream reach downstream of the measurement location until the next station or the mouth into the main river. In all of the important stream reaches, water level loggers could be installed at least at one location close to the mouth of the stream reaches into the main river and at one location upstream close to the alluvial aquifer borders. If an official gauging station was present upstream (such as at the Rotbach tributary or in the Brugga tributary), no additional station was installed upstream.

In practice, many practical limitations to possibilities for installation existed (option to fix equipment, private/public property

situation, etc.). The image-based method with QR-code panels was only used in locations where the panels could be deployed on a vertical surface. These were either large rocks or bridges, weirs or small hydroelectric power plants. Settings differ with regard to light conditions and shape or size of the river sections. In order to investigate the effect of light reflections on the output of the image-based method, some of the cameras were placed below bridges. Furthermore, care was taken that the panel position was vertical and, that the distance between the panel and the camera was adequate to maintain the necessary image resolution (<5 m). The position of the camera was adjusted as such that the panel was portrayed in the centre of the image. However, due to the manual maintenance of the cameras and the influence of the natural environment, it was not guaranteed that the position remained exactly the same during the whole measurement time span. At each measurement location additional staff gauges were installed. Water levels are logged by Ody and QR WLL with a temporal resolution of 15 min.

4 | RESULTS

4.1 | Comparison of the measured water levels

First, both WLL methods are compared with regard to their application and operability based on the operational time, time and effort for installation and processing of the data. The Ody data was processed with the Odyssey Software (Ltd, 2012). Processing of the QR images took significantly longer, but is not possible to obtain the time needed for reading one image with QR because the number of QR codes detected per image varies according to water level and error sources. For example, reading of 100 images took 1.57 min with an Core i7 processor. The effort for the installation was comparable for both methods. Overall, the maintenance cost was higher for the image-based method due to the energy consumption of the camera set at high resolution. A battery with an electric charge of 4.5 Ah was sufficient to keep the cameras running for approximately 1 month in winter and 2 months in summer on average. According to the manufacturer of the Ody loggers, the battery life is >9 months. Thus, battery replacement and data collection needs to be done at higher frequency for the QR method. On the other hand, the maintenance cost and effort for the QR measurements was high due to manual verification of the image section, the manual data collection and regular replacement of the memory cards.

The data sets obtained with the different measurement methods differ with regard to data availability and completeness of the time series, data quality and consistency of the measured water levels. The data measured by the monitoring system was processed for the time period between June and October 2020. The density distributions of all water levels measured during the study period at each station vary (Figure 4). Whereas the violin plot of some locations is multimodal or bimodal (K1, W4, B2, E4, E2), the distribution is unimodal for other locations (E6, E8). For some locations (e.g., K1, RE1, E4), the shape of the distribution differs depending on the measurement method used. The violin plots indicate that where the shape of the violin of the Odyssey and QR code data are more alike (E8, E6),low water levels occur at higher frequency in the Odyssey data set, except for B2 and RO2B. In general, there are more outliers in the QR code data set in high water levels. The percentage of available data per station is considerably lower for the QR data in comparison to the Ody data (Figure 5b). More than 50% of data was missing at some locations (i.e., at RO2A, RO2B and E2). Additionally, the temporal evolution of the water levels (15 resolution) between June and October 2020 at each measurement location is analysed (Figure 5a). While the water level remains constant at some locations during the measurement period (i.e., constantly high water levels at RO2B and constantly low water levels at E6 and E8), other locations show stronger fluctuations and in some cases also a stronger tendency for low water levels to occur in the summer months (i.e., D2, E2, W4). Furthermore, the range of water levels measured with the Odyssey method suggests that the closer the stations are to the outlet of the catchment, the lower are

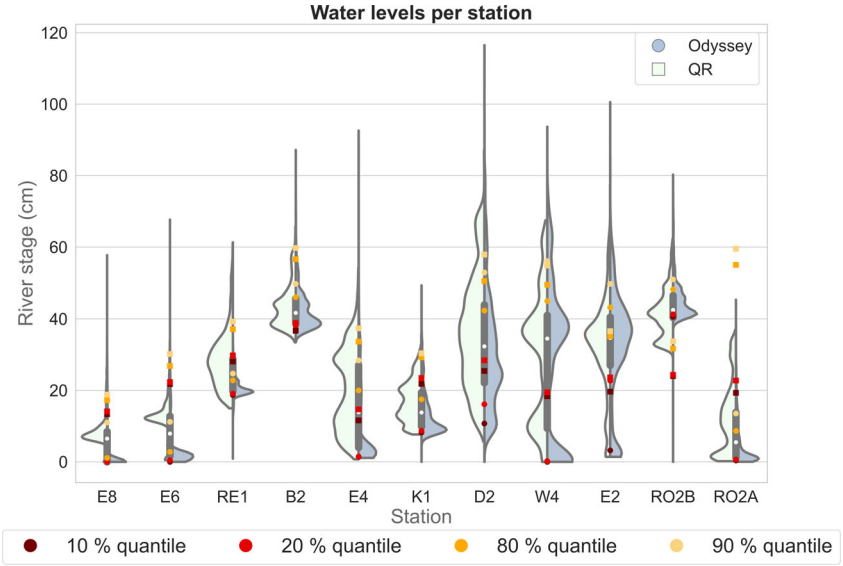

FIGURE 4 Distributions of all measured water levels per station for both measurement methods. Measurement locations are sorted left to right with increasing distance from the catchment outlet

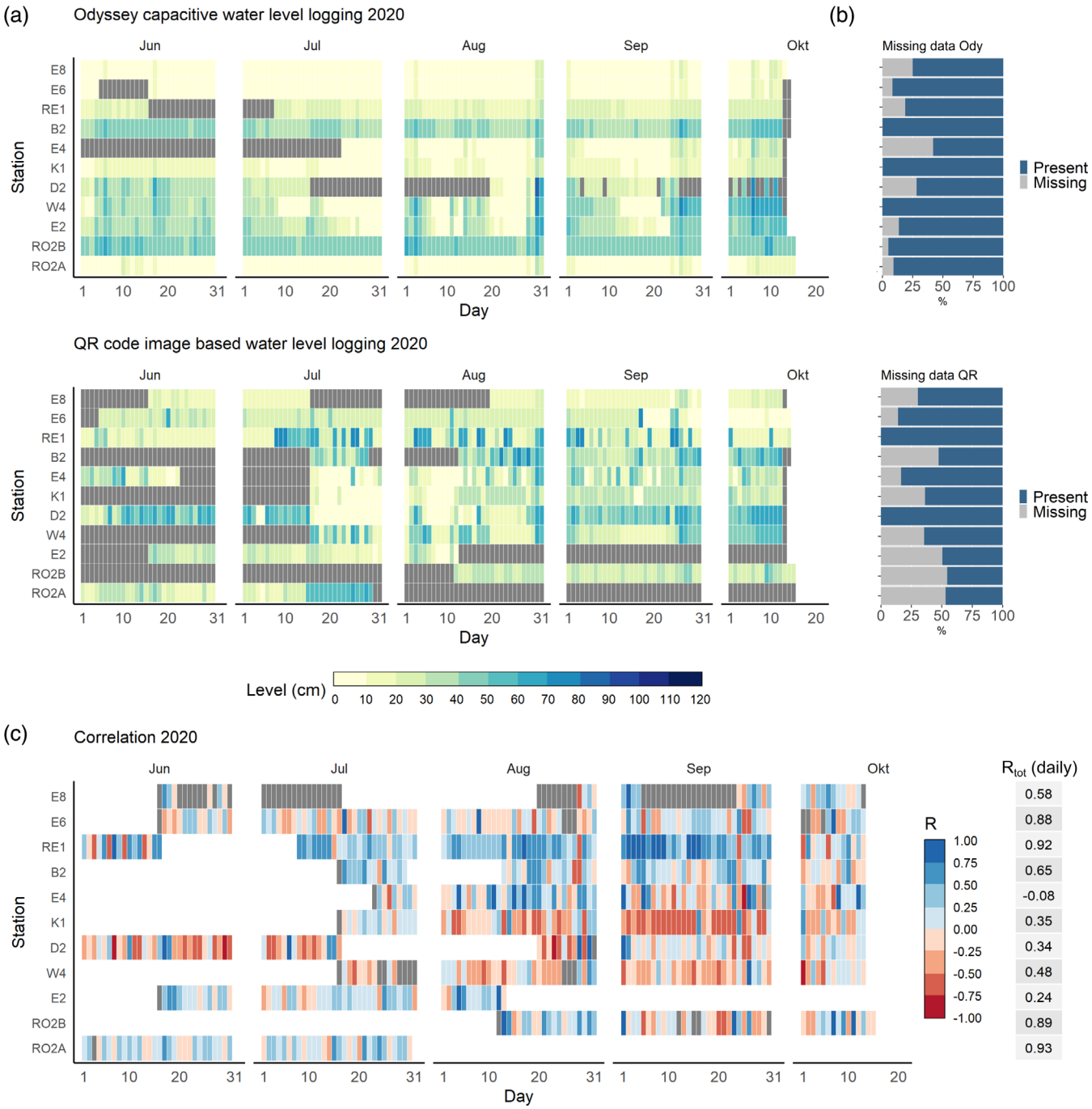

FIGURE 5 Data availability and rolling R for Ody and QR water levels. (a) The range of water levels measured with each of the methods. (b) Percentage of available data per method and measurement station. (c) The rolling R for both measurement methods

the water levels in general. The further away the measurement locations are from the catchment outlet, the stronger are the fluctuations. With regard to the distance from the catchment outlet, the QR code measured water levels do not show any clear differences(Figure 5a). In general, fast changes from low to very high water levels occur more often in the QR water level time series (i.e., RE1).

The rolling correlation shows, that there is no clear relation of Ody and QR measurements (Figure 5c). Exceptions are RE1 and K1. At RE1, a relation of both measurements appears for most of the days. In some locations (i.e., K1) even a negative relation exists, meaning that the Ody water levels increase (decrease) while QR water levels decrease (increase). Note, that *R* cannot be calculated for a standard deviation (STD) of 0, which is the case when zero water level occurs over longer time windows than a day (e.g., at E8, E6 and W4). We also calculated R using a rolling mean with a window width of 1 day (96 steps) and the daily means for each station (Figure 5c R_{tot}). For daily resolution we find higher R_{tot} (e.g., at RO2B, RO2A, E6 and RE1). At some stations however, the number of dates when QR

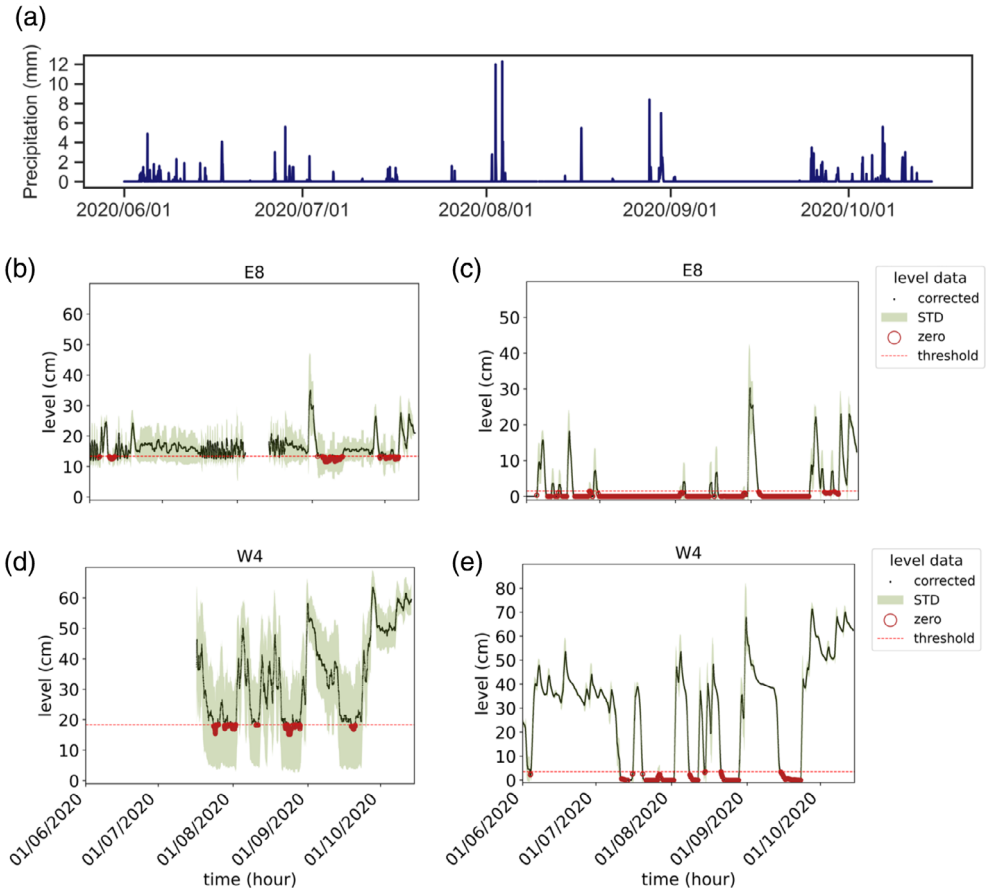

FIGURE 6 Precipitation from the DWD (a) and Hydrographs with 15 min water levels of QR (b, d) and Ody (c,e) measurements in summer 2020 at two measurement stations of the Wagensteigbach and Eschbach river reach. Corrected data is displayed in black and the Standard deviation is shaded. The zero water level occurences and the threshold is shown in red.

measurements and Ody measurements are available is very low (61 days only at RO2B, 65 days only at RO2A).

4.2 | Hydrographs

The hydrographs (15 min resolution) of the Ody and QR measurements show the different temporal dynamics at different locations along the stream reaches (Figure 6b–e blue lines. More hydrographs are shown in the Figure A4 and A5 in Data S1). Ody data was corrected using the mean of the minimum in the water level time series for all stations, which was 5 cm (Figure 6c,e black points; see section 2.3). In the Ody hydrographs at locations E8 in the Eschbach and W4 in the Wagensteig tributaries, a time span with constantly (slope close to zero) very low water levels below 5 appears several times in between the peaks in the course of the study period (Figure 6c,e). Water level rise often occurs shortly after rainfall events (Figure 6a), as expected due to the fast reacting character of the hydrological system (Uhlenbrook, 1999; Wissmeier & Uhlenbrook, 2007). The QR hydrographs reflect the same general pattern as the Ody hydrographs but with more outliers towards higher water levels. Longer time spans with constantly low water levels are not visible in the QR hydrographs. Instead smaller, high frequency fluctuations occur in between the marked peaks while water levels rarely drop below 10 (Figure 6a, c). The spread in the rolling STD is also noticeably smaller for the water levels measured with the Ody method (water levels are less scattered), regardless of the temporal resolution (15 min, hourly or daily). All in all, the hydrographs show, that water levels measured via QR tend to be overestimated in comparison to the Ody data (despite QR measurements being limited to 73 cm), similar to what the range of water levels in Figures 4 and 5 indicates.

The different results of Ody and QR code measurements can be explained by looking at different error sources that are typical for image-based measurements of water levels. After visual inspection of the images in our data set, we identified sediment accumulation on the panel, light reflections and overexposure as the major error sources (Figure A1 in Data S1). Overexposure occurs in locations, where the angle between QR code panel and the sun is particularly unfavourable at a certain time during the day. This effect of back radiation can be enhanced by the colour of the panel background and higher roughness of the panel surface. Light reflections are mostly caused in places, where the interaction of sun light and leaves of trees or other plants create a pattern of light and shadow on the panel. Sediment accumulation is caused by the deposit of organic material on the panel at and below the water surface. When the river bed dries, the deposits dry, remain on the panel and conceal a part of the QR codes. The three error types are caused by the local environment. We therefore focused on errors due to local environment for pre-and post processing of the images (see section 2.2).

TABLE 3 Total number of measured values (*N*) and percentage of zero level occurences per month

Month 2020	May	Jun	Jul	Aug	Sept	Oct	May	Jun	Jul	Aug	Sept	Oct
Stations	*N*						Percentage (%)					
B2	434	2880	2976	2976	2880	1217	-	-	-	-	-	-
D1	0	0	731	2976	2880	1212	-	-	-	-	-	-
D2	533	2880	1496	1001	2081	593	-	-	-	76	2	-
D3	0	0	0	1011	2880	1202	-	-	-	9	54	-
E2	516	2880	2976	2976	2880	1208	-	-	9	28	1	-
E4	0	0	1149	3912	2880	1206	-	-	61	48	-	-
E6	512	2880	2963	2975	2880	1203	-	23	58	43	19	-
E8	509	2880	2977	2975	2880	1201	-	36	100	68	66	33
IB1	123	2580	2666	2855	2880	1344	-	-	-	30	14	-
IB2	134	2580	3613	3342	2864	1344	-	-	8	9	-	-
K1	436	2882	2975	2976	2880	1215	-	-	-	-	-	-
RE1	136	1494	2254	2976	2880	1220	-	19	-	-	-	-
RO2A	250	2880	3761	4464	4320	2016	-	21	69	31	23	-
RO2B	250	2880	2976	3906	4320	2016	-	-	-	-	-	-
W1	137	2580	3613	3531	2880	1344	-	-	-	-	-	-
W2	156	2880	3614	4465	2952	1344	-	7	30	16	-	-
W3	135	2580	3614	4464	4319	2016	-	-	11	5	-	-
W4	246	2880	2975	2976	2880	1310	-	0	33	29	24	-
ZA1	140	2880	3763	4464	4320	2016	-	-	-	-	-	-

4.3 | Zero level occurrences

With the Ody data set we analysed zero level occurrences for all stations along the tributaries. Zero level occurrences were selected from the Ody data based on a threshold value and a rolling coefficient of variation (see also section 2.3). In Figure 6b–e, the hydrographs, the threshold and the selected zero level occurrences in the time series (highlighted in red) are shown for the two locations with different dynamics at the Eschbach tributary (E8) and the Wagensteigbach tributary (W4) (see also Figure 3). E8 represents an example with particularly long dry phases, whereas dry phases occuring at W4 are significantly shorter and transition times from high to low water levels are faster. As time lapse cameras and Ody loggers were closely installed and the river bed and loggers are on the images in most cases, it was assumed that the images from the time lapse cameras can be used for validation of the zero level occurrences (see section 2.2). However, due to the high temporal resolution of 15 min, the visual inspection of images at locations where the riverbed is prone to run dry frequently and for several days requires tremendous time and effort. For E8, this would have required to visually inspect 8323 images. Therefore, a random choice of 10% of the images (corresponding to zero for false positive and to no zero water level occurences for false negative errors) were validated. The riverbed was classified as dry (not dry) for 100% (48%) of the images at E8 and for 100% (85%) of the images at W4 corresponding to Ody zero water levels (corresponding to no zero water levels). While false positive errors remain sparse, there is a tendency for false negative errors to occur at E8. A possible explanation is, that the catchment-specific threshold chosen for zero water level selection leads to underestimation of zero water level occurrences at this specific location. Despite this underestimation at specific locations, the validation illustrates, that the selection of zero level occurrences is robust in general (Table 2 in Data S1).

Hence, an analysis and inter-comparison of the total zero level occurrences per month of the different locations for the measurement period between June and October 2020 is feasible. The same methodology for zero water level filtering was applied to all other locations in the catchment (see Figure A7 in Data S1. All locations with Ody loggers are included as shown in Figure 3). An overview of the monthly percentage of zero occurrence is given in Table 3 for the Ody data set. The percentage of zero level occurrence is calculated based on the total number of values N that was measured at each location per month.

Zero water levels begin to occur in June 2020 and increase throughout July and August as the severity of the hydrological drought increases at a number of locations with zero flows over longer time periods (Figure 7). E8 was dry for 100% of the time in July, 68% in August and 66% in September (Figure 7). In September, zero level occurrences start to decrease again and most locations recover from the drying until October 2020, when E8 remains the only station where the riverbed is still partially dry. In general, this pattern indicates, that especially the northwestern stream reaches of the study area are prone to drying out (see also Figure A2 in Data S1). Additionally, a longitudinal drying pattern emerges along the Eschbach river, as

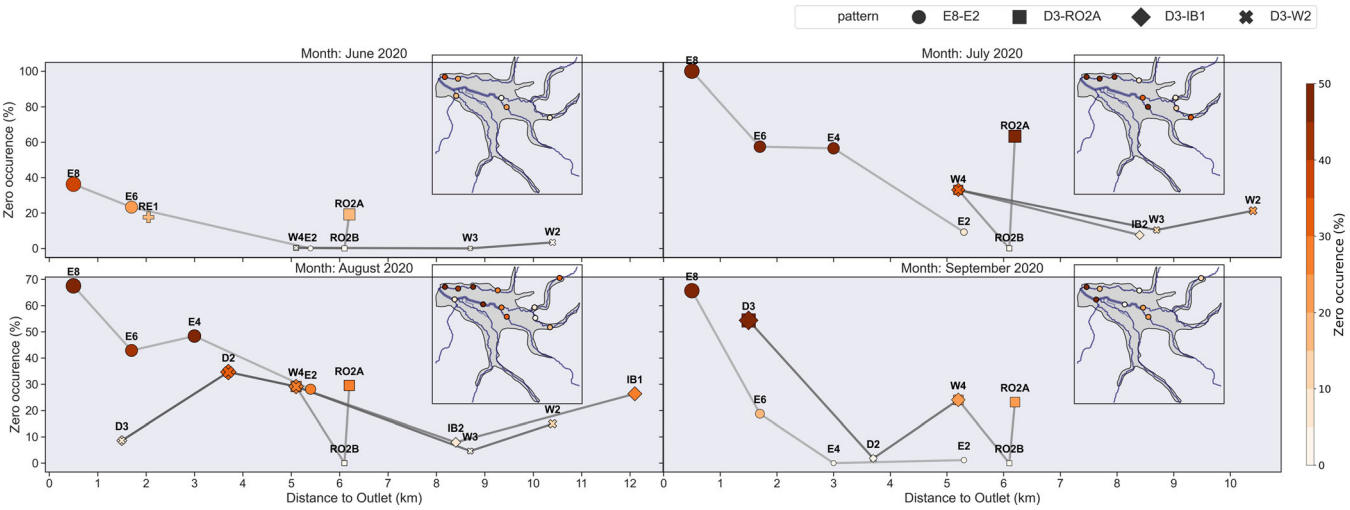

FIGURE 7 Total monthly zero water level occurences per measurement location in percent for the Ody data and the longitudinal drying patterns determined from the percentage of Ody zero water level occurences of each month. The colour and size of the markers represent the percentage of zero water level occurences.

downstream stations dry out first and upstream stations follow later in July and August (Figure 7). Nevertheless, streams in the central part of the catchment also show relatively high monthly percentage of zero levels from July to September. The south western parts of the catchment are least prone to drying out.

The mean monthly percentage of zero occurrences along the tributaries represent typical but different longitudinal drying patterns (Figure 7). Zero flows are mostly more frequent for the downstream stations close to the outlet (distance in km along the river network) and decrease in the upstream direction >8 km. The only exception is RO2A, which is experiencing relatively high zero flow occurrence on average even though it is located at medium distance from the outlet. However, clear longitudinal trends do not occur at all stations and change points in the longitudinal profiles indicate local influences on hydrological dynamics. Regarding the temporal evolution during the summer of 2020, four different patterns emerge with (1) relatively high zero occurrence increasing throughout summer and decreasing slightly towards the end of summer (E8, E6, E4, RO2A, W4); (2) high zero occurrence at the beginning of summer and no or decreasing zero occurrence afterwards (RE1); (3) zero occurrence increasing towards the end of summer (D3, D2) and (4) relatively low number of zero occurrence or only increasing slightly during summer (W3, W2, IB1, IB2, B2). Type (4) patterns are mostly experienced by the upstream stations, which indicates that they are in general less affected by drying than downstream stations.

In order to estimate the difference between zero water levels based on Ody and QR, the percentage change $\left(\frac{\left(x_{ody}-x_{qr}\right)}{|xody|}^{*}100\right)$ between Ody and QR zero water level occurrences was calculated (for the locations with data of both measurement methods; see also Figures A3 and A6 in Data S1). At most locations, the percentage of zero levels measured with the Ody data surpasses the percentage of zero levels measured with the QR data in July and August (strongest for the Eschbach tributary with a percentage change of $> 90\%$).

5 | DISCUSSION

5.1 | Technical challenges of QR code based WLL

In this this study we tested a new experimental setup to measure water levels with the the QR method in a natural environment and with a focus on zero flow identification. We used QR codes as fiducial markers because of readily available software. However, other fiducial markers may also be well suited for water level measurement (Fiala, 2010; Kalaitzakis et al., 2021). Different error sources of QR WLL limit the use and impact the uncertainty of the measurements and led especially to overestimation of low water levels in comparison to the Ody WLL method. Future application of QR WLL may improve the setup based on our findings. Firstly, the accuracy of the QR WLL is limited to (3 cm) due to the size and arrangement of the QR codes on the panel. This accuracy is not sufficient for water level measurements according to the guidelines of the federal state of Baden Württemberg (LAWA, 2018) and to develop rating curves. Also, this relatively coarse resolution leads to higher risk of positive outliers if more than one QR code cannot be read. In general, the image resolution is dependent on the focal length of the camera or image, the size of and the distance between the QR codes (Gilmore et al., 2013). Thus, an application of the method in other streams with larger widths may be limited, due to a decreasing image resolution with increasing distance between the camera and the panel (even though this also depends on the camera used). In our setting, a key aspect was to find a low-cost solution, that is easily applicable and also holds potential for the use in citizen science. It is therefore expected, that better photographic equipment and better image resolution could be beneficial for QR-code recognition. Hence, the error sources that were identified with our measurements in a natural environment (see Figure A1 in Data S1) might be reduced with experiments with varying technical setups in laboratory environment in order to find the smallest

resolution possible to deliver valuable results. Underwater detection of fiducial markers might also be an issue, although this likely occurs under very specific conditions (Čejka et al., 2019; dos Santos Cesar et al., 2015). Problems with sediment accumulation and with different illumination could be reduced using different panel coatings but those need to be bio-compatible as they should not be harmful to other organisms in the aquatic ecosystem. The occurrence of light reflections is also strongly controlled by smoothness of the panel surface. The smoother the surface, the more reflections will occur. On the other hand, a smooth surface provides less favourable conditions for strong sediment accumulation than a rough surface. Light reflections are also a result of the postion of the panel and the position of the sun and therefore always occur for a certain duration and not permanently. Few light reflections occur likely at the beginning (when the disturbance due to sunlight starts) and at the end (when the disturbance due to the sunlight stops) of the time during which light reflections or overexposure occur in general. Problems with over exposure and light conditions may also be avoidable if the geographical orientation of the measurement location is taken into account in locations without much vegetation cover (a North oriented panel is likely not as much affected by sunlight as a South, West or East oriented panel).

We have also shown that a distinction between different error sources by means of simple, automatic image-processing techniques is not yet possible (Figure 2). Such a method could either be applied to pre-select images affected by error sources or to remove wrong values in the time series using the time stamp of the erroneous image afterwards. Using an automatic thresholding algorithm, it was possible to identify overexposure and strong light reflections while it was not possible to distinguish between normal conditions and few light reflections or sediment accumulation. To reliably filter erroneous images in a pre-or post-treatment, image-processing techniques still need to be improved with a focus on different degrees of light reflections and sediment accumulation. An algorithm, that compares the threshold of a particular image to the prior or following image taken could probably be useful to identify the beginning and the end of the light reflections automatically. Further refinement of the approach could consist in using mean values of the pixel percentage P_{pix} for all images belonging to the specific error groups and all normal images of one station instead of using benchmark images only. The regions and P_{pix} given in Table 2 are site-specific (here for the station E4) and needs to be defined for every measurement location in order to finally apply pre- or post-processing. A simple Otsu-thresholding algorithm is not sufficient to filter erroneous images. There may be other image processing techniques that could be applied but it was out of the scope of this study to develop a new methodological approach.

Certainly, there is a need to compare the performance of different algorithms. So far (Zhang et al., 2019) compared Order-Statistic-Filtering (OSF) to Otsu-thresholding for water line detection and achieved better results during foggy and rainy conditions but not during sunny conditions (which are the main reason for light reflections). Up to date, image processing cannot compensate for refinement of the experimental design to avoid the above-mentioned problems.

Despite deliberate maintenance, several data gaps appear in our QR dataset (Figure 5). A possibility to reduce maintenance cost for both methods is to use cameras or data loggers with automatic data transmission for long-term monitoring to simplify data collection, troubleshooting and to avoid deficiency of the devices for longer time periods. However this requires either more financial resources or problems related to the energy consumption of self-made automatic data loggers based on Raspberry PI systems need to be solved first. For example, (Eltner et al., 2018) used a car battery to obtain data with 30 min to 1 h resolution. Furthermore, data transmission with such data loggers only works in areas with mobile coverage and such sensors may be sensitive to temperature as well, as it was shown by Elias et al. (2020) in combination with smartphone cameras.

5.2 | Measurement comparison

The quality and the amount of the data obtained with the QR method is lower while the data handling is also more complicated in comparison to the data obtained with capacitive water level logging. We therefore assumed that the data obtained with the Odyssey loggers is more reliable for an analysis of zero levels. Specific for the measurement of zero water levels, the combination of the general error sources when using image based measurements and the use of QR codes as fiducial marker may lead to an overestimation of low water levels at a specific resolution. This should be kept in mind when developing such image based methods using fiducial markers further—particularly for citizen science applications. While the use of QR may reduce uncertainty due to subjectivity when interpreting the information on stage height contained in images visually, the flow state cannot be measured directly without making the assumption that the presence of water automatically indicates flow as well (at least not using an automatic algorithm). Thus, this is one of the shortcomings of the Ody method with respect to application in IRES. Therefore, it is essential to compare the Ody with other measurement methods. Those could also be electrical resistance measurements, which have also been successfully used for monitoring of the aquatic states of IRES (Assendelft & van Meerveld, 2019; Bhamjee et al., 2016; Blasch et al., 2002; Chapin et al., 2014), ultrasound and radar technologies, which are also commonly used in hydrometry (LAWA, 2018) or even image-based information if the flow state is assigned manually (Kaplan et al., 2019, 2020).

Furthermore, the correlation analysis revealed partial contradictory behaviour of QR and Ody measurement, which impeded complementary usage/merging of the two data sets. Nevertheless, the combination of the logged water levels and the visual data contained in the images from the QR-codes provides several advantages. On the one hand, it allows to check for external confounding factors in the river bed or the local environment that may influence measurements. On the other hand, the information contained in the image was useful for validation of the Ody measurements. The sensitivity of the Ody measurements to soil moisture could also result in a time lag between the true occurrence of zero water level and the actual recorded zero

water level. This was not taken into account in this study but a complementary use of Ody and image-based information also yields potential for an identification of the time lag.

A huge effort for image processing is necessary in comparison to the capacitive water level measurement. The quality of the result dependends on the image processing software used. Advanced image processing methods solve specific problems and are often developed for medical purposes and measurements under stable (laboratory) conditions. Kaplan et al. (2019) used the open source software ImageJ (Schneider et al., 2012) and new image processing techniques and machine learning algorithms (neural networks) are further developed in order to identify specific patterns and might also deal with natural conditions for hydrological purposes (Eltner et al., 2021; Ljubičić et al., 2021). Convolution neural networks have been found to be more robust to environmental conditions (Eltner et al., 2018, 2021), in agreement with our findings that light conditions are, among others, a major error source. We conclude that error sources have now been well identified, but that the solutions from an image treatment or artificial intelligence perspective have not yet been solved. This implies that up to date, particular care needs to be taken regarding the choice of measurement locations when working with image-based technologies (particularly in environments with tree shading).

5.3 | Confidence and interpretation of zero level occurrences

We successfully validated zero level occurrences based on the Ody data using images of the river bed. False negative errors slightly exceeded false positive errors, which indicates that zero water level occurrences are likely underestimated and not overestimated.

The thresholds and constraints (CV <0.1 for 4 h) used are specific for the study catchment in general but they are not specific for each measurement location. A generalization of these constraints for catchments of larger size requires further research because the dynamic behaviour of the river reach has to be taken into account (long dry periods vs. short dry periods). In a specific location where fast fluctuations are likely to occur, the time threshold should be smaller. If it is likely that the riverbed dries over longer periods at specific locations, a larger time threshold could be a better choice. The use of generalized criteria for the whole catchment lead to a higher amount of false positive errors at locations, where standing water predominates (RO2A, E6, E4) and to false negative errors at locations where zero water level predominates (E8) throughout the summer months. A very particular case with remaining low water levels during the whole summer was RO2A (according to visual inspection of the images of the false positive validation this concerned 100% of the images, where no flow and thus standing water was found). The latter shows, that information on all aquatic states is extremely relevant also for the identification of zero water level. In general, the approach of zero water level selection could benefit from a definition of thresholds and criteria specific to each stream reach or location.

Zero level or intermittency occurrence has often been validated using data from field mapping campaigns (e.g., Durighetto et al., 2020; Godsey & Kirchner, 2014; Goulsbra et al., 2014; Jensen et al., 2017; Jensen et al., 2019; Lovill et al., 2018; Olson & Brouillette, 2006; Shaw, 2016; Shaw et al., 2017; Whiting & Godsey, 2016; Zimmer & McGlynn, 2017). Our results show that validation with image-based measurement methods is a promising alternative and helps to identify potential uncertainties in consequence of the threshold chosen. The validation of zero level occurrences also yields further potential for the application of deep learning techniques to identify zero water levels from the images. Under the assumption that zero water levels measured with the Ody loggers are also represented by the information contained in the images, similar data sets could be used as training and validation data.

Altogether, the analysis of zero level occurrences denotes, that the obtained data set is suitable for an event based analysis of zero water level events in our example catchment. We were able to identify the longitudinal drying patterns per month in different stream reaches in the Dreisam valley between June and October 2020 and to show that there are spatio-temporal differences of the occurrence of zero water level at different locations (Figure 7). The spatiotemporal evolution of the longitudinal drying suggests a top-down connectivity in most of the river reaches (Goulsbra et al., 2014; Peirce & Lindsay, 2015) because dry conditions occur earlier and at the downstream locations, while more water is still present in early summer and also refills earlier at the end of summer at upstream locations (Figure 7). This decreasing drying downstream is particularly observed in the northern part of the catchment (Eschbach). The plots suggest that the drying in the main river occurs later potentially due to the lower contributions of the river reaches in late summer. However, the interpretation of the spatio-temporal pattern of the main river is hampered by the low amount of data at D3 in July (Table 3). Even though less zero water levels occur in the upper tributaries (Ibenbach, Wagensteigbach, Rotbach), the pattern indicates bottom-up connectivity. These differences could in part be explained by physiographic characteristics. In the deep valley aquifer surface water- groundwater interactions can cause changes from infiltrating to exfiltrating conditions. In contrast, the Ibenbach, Wagensteig and Rotbach tributaries follow narrow valleys with less groundwater for exchange but they are closer to high-elevation headwaters with generally more subsurface contributions from hillslopes (Uhlenbrook et al., 2002, 2004). The contradictory situation at RO2A and RO2B despite the short distance is most likely caused by water usage (there is a weir discharging water for hydropower generation in vicinity of the stations). Exceptions with no or very low amount of zero water levels are the downstream locations at the Reichenbach (RE1), Brugga (B2) and Zastler (K1) tributary.

The drying patterns in Figure 7 are exemplary for this data set obtained and allow the development of hypotheses on the hydrological processes. However, while the results of this study are restricted by the measurement uncertainties and by the different lengths of the time series measured per month, they provide an outlook what could be gained from a more complete longitudinal temporal profile in terms of process understanding. To pursue a classification of the stream

network into ephemeral, intermittent or perennial, there is a need to collect data of the entire hydrological year and of streamflow data for further analysis of the spatio-temporal behaviour of intermittent streams (for example in order to use active stream length vs. discharge relationships (Shaw et al., 2017; Zanetti et al., 2022) or to differentiate between different origins of hydrological flow (Zimmer & McGlynn, 2017)). For the measurement methods used in this study, rating curves (the relationship to calculate discharge as a function of recorded water levels) need to be developed to obtain discharge data. The generation of such rating curves could be a next step to estimate the contribution of each of the stream reaches to the main river and to quantify the amount of water that is missing once different stream reaches dry up. This is an essential step for the assessment of different control factors for the observed spatio-temporal patterns, especially in the context of an altered river system (with water abstraction and hydroelectric power generation).

6 | CONCLUSION

This study evaluated the potential of an image-based measurement method using time lapse cameras and QR-codes as fiducial marker compared to a capacitive measurement method for measuring zero water levels in a meso-scale catchment with temperate climate in South Western Germany. We found, that the largest errors using image-based measurements were due to the local environment. The available open source QR code readers were not able to distinguish between images affected by such errors (i.e., light reflections due to patterns of light and shadow or due to the water surface and sediment accumulation) and a normal image. Where overexposure or sediment accumulation occurs, the information on the fiducial marker is lost leading to wrong measurement results. Therefore, image processing can only be used in order to exclude the erroneous images prior to QR code recognition with a software. We experienced, however, that a simple algorithm for automatic thresholding is not sufficient in order to account for error sources due to the natural environment. Thereby, we conclude, that the choice of the measurement location is extremely important when working with image-based methods, especially if stream reaches are partially tree-shaded. To effectively monitor IRES using combinations of image-based measurements and other methods, image-processing needs to be improved specific for errors due to the natural environment. Due to the above mentioned error sources and the high efforts for maintenance and data handling, the data obtained with the image-based method could not be used alone for an analysis of zero level occurrences. The analysis of zero level occurrences between spring and autumn 2020 using the data of the capacitive measurement method showed the potential of such measurements to gain insight into drying patterns and processes. To obtain information on longitudinal connectivity it was crucial to disentangle the drying dynamics of the different tributaries. Monitoring approaches should therefore at least focus on the scale of tributaries (and not only on the catchment-scale) to study IRES processes in detail.

ACKNOWLEDGEMENTS

The authors acknowledge the work of Britta Kattenstroth and Jonas Schwarz for their help with the technical equipment of the measurement locations. Verena Völz also assisted with data collection in 2020. Furthermore, we acknowledge the valuable contribution of Klaus Meyer for his work on trial measurements with the initial setup of the QR code based water level loggers during his MSc Thesis (Meyer, K. 2019. Monitoring of low flow regimes in the Dreisam valley using flexible gauging stations. Master Thesis. University of Freiburg). Open Access funding enabled and organized by Projekt DEAL.

FUNDING INFORMATION

Badenova Fund For Innovation.

CONFLICT OF INTEREST

The authors declare no conflict of interest.

DATA AVAILABILITY STATEMENT

The measurement data that support the findings of this study are published in FreiDok repository (https://doi.org/10.6094/UNIFR/228702)

ORCID

Amelie Herzog https://orcid.org/0000-0002-1454-0345
Markus Weiler https://orcid.org/0000-0001-6245-6917

REFERENCES

Abeles, P. (2013). Examination of hybrid image feature trackers. In *International Symposium on Visual Computing (ISVC)*.

Abeles, P. (2016). Boofcv v0.25. http://boofcv.org/.

Abeles, P. (2018). Study of qr code scanning performance in different environments. v3. https://boofcv.org/index.php?title=Performance:QrCode.

Abeles, P. (2021). Pyramidal blur aware x-corner chessboard detector. *ArXiv*, *abs/2110.13793*.

Acuña, V., Jorda-Capdevila, D., Vezza, P., de Girolamo, A. M., McClain, M. E., Stubbington, R., Pastor, A. V., Lamouroux, N., Schiller, D., Munné, A., & Datry, T. (2020). Accounting for flow intermittency in environmental flows design. *Journal of Applied Ecology*, *57*(4), 742–753.

Assendelft, R., & van Meerveld, H. (2019). A low-cost, multi-sensor system to monitor temporary stream dynamics in mountainous headwater catchments. *Sensors (Basel, Switzerland)*, *19*(21), 1–28.

Bhamjee, R., Lindsay, J., & Cockburn, J. (2016). Monitoring ephemeral headwater streams: A paired-sensor approach. *Hydrological Processes*, *30*(6), 888–898.

Blasch, K., Ferré, T. P. A., Christensen, A., & Hoffmann, J. (2002). New field method to determine streamflow timing using electrical resistance sensors. *Vadose Zone Journal*, *1*(2), 289–299.

Blauthut, V., Fleischer, C., and Stölzle, M. (2017). *Pilotstudien zum Niedrigwassermanagement in Baden-Württemberg*. LUBW - Landesanstalt für Umwelt, Messungen und Naturschutz, Baden-Württemberg.

Botter, G., & Durighetto, N. (2020). The stream length duration curve: A tool for characterizing the time variability of the flowing stream length. *Water Resources Research*, *56*(8), e2020WR027282.

Botter, G., Vingiani, F., Senatore, A., Jensen, C., Weiler, M., McGuire, K., Mendicino, G., & Durighetto, N. (2021). Hierarchical climate-driven dynamics of the active channel length in temporary streams. *Scientific Reports*, *11*(1), 21503.

Bruinink, M., Chandarr, A., Rudinac, M., van Overloop, P.-J., & Jonker, P. (2015). Portable, automatic water level estimation using mobile phone cameras. In *IAPR MVA 2015* (pp. 426–429). Institute of Electrical and Electronics Engineers.

Čejka, J., Bruno, F., Skarlatos, D., & Liarokapis, F. (2019). Detecting square markers in underwater environments. *Remote Sensing*, *11*(4), 459.

Chapin, T. P., Todd, A. S., & Zeigler, M. P. (2014). Robust, low-cost data loggers for stream temperature, flow intermittency, and relative conductivity monitoring. *Water Resources Research*, *50*(8), 6542–6548.

Chapman, K. W., Gilmore, T. E., Chapman, C. D., Mehrubeoglu, M., & Mittelstet, A. R. (2020). Camera-based water stage and discharge prediction with machine learning. *Hydrology and Earth System Sciences Discussions*, *2020*, 1–28.

Costigan, K. H., Jaeger, K. L., Goss, C. W., Fritz, K. M., & Goebel, P. C. (2016). Understanding controls on flow permanence in intermittent rivers to aid ecological research: Integrating meteorology, geology and land cover. *Ecohydrology*, *9*(7), 1141–1153.

Datry, T., Bonada, N., & Boulton, A. J. (2017). *Intermittent rivers and ephemeral streams: Ecology and management*. Academic Press.

Döll, P., & Müller Schmied, H. (2012). How is the impact of climate change on river flow regimes related to the impact on mean annual runoff? A global-scale analysis. *Environmental Research Letters*, *7*(1), 014037.

dos Santos Cesar, D. B., Gaudig, C., Fritsche, M., dos Reis, M. A., & Kirchner, F. (2015). An evaluation of artificial fiducial markers in underwater environments. *OCEANS 2015* (pp. 1–6). IEEE.

Durighetto, N., Vingiani, F., Bertassello, L. E., Camporese, M., & Botter, G. (2020). Intraseasonal drainage network dynamics in a headwater catchment of the italian alps. *Water Resources Research*, *56*(4), 1–22.

Elias, M., Eltner, A., Liebold, F., & Maas, H.-G. (2020). Assessing the influence of temperature changes on the geometric stability of smartphone- and raspberry pi cameras. *Sensors (Basel, Switzerland)*, *20*(3), 643.

Eltner, A., Bressan, P. O., Akiyama, T., Gonçalves, W. N., & Marcato Junior, J. (2021). Using deep learning for automatic water stage measurements. *Water Resources Research*, *57*(3), e2020WR027608.

Eltner, A., Elias, M., Sardemann, H., & Spieler, D. (2018). Automatic image–based water stage measurement for long–term observations in ungauged catchments. *Water Resources Research*, *54*(12), 10–362.

Erfurt, M., Skiadaresis, G., Tijdeman, E., Blauhut, V., Bauhus, J., Glaser, R., Schwarz, J., Tegel, W., & Stahl, K. (2020). A multidisciplinary drought catalogue for southwestern Germany dating back to 1801. *Natural Hazards and Earth System Sciences*, *20*(11), 2979–2995.

Etter, S., Strobl, B., van Meerveld, I., & Seibert, J. (2020). Quality and timing of crowd–based water level class observations. *Hydrological Processes*, *34*(22), 4365–4378.

Fiala, M. (2010). Designing highly reliable fiducial markers. *IEEE Transactions on Pattern Analysis and Machine Intelligence*, *32*(7), 1317–1324.

Fortesa, J., Ricci, G. F., García-Comendador, J., Gentile, F., Estrany, J., Sauquet, E., Datry, T., & de Girolamo, A. M. (2021). Analysing hydrological and sediment transport regime in two mediterranean intermittent rivers. *Catena*, *196*, 104865.

Fovet, O., Belemtougri, A., Boithias, L., Braud, I., Charlier, J.-B., Cottet, M., Daudin, K., Dramais, G., Ducharne, A., Folton, N., Grippa, M., Hector, B., Kuppel, S., Le Coz, J., Legal, L., Martin, P., Moatar, F., Molénat, J., Probst, A., … Datry, T. (2021). Intermittent rivers and ephemeral streams: Perspectives for critical zone science and research on socio–ecosystems. *WIREs Water*, *8*(4), e1523.

Gallart, F., Cid, N., Latron, J., Llorens, P., Bonada, N., Jeuffroy, J., Jiménez-Argudo, S.-M., Vega, R.-M., Solà, C., Soria, M., Bardina, M., Hernández-Casahuga, A.-J., Fidalgo, A., Estrela, T., Munné, A., & Prat, N. (2017). Trehs: An open-access software tool for investigating and evaluating temporary river regimes as a first step for their ecological status assessment. *The Science of the Total Environment*, *607-608*, 519–540.

Gilmore, T., Birgand, F., & Chapman, K. (2013). Source and magnitude of error in an inexpensive image-based water level measurement system. *Journal of Hydrology*, *496*, 178–186.

Gleason, C. J., & Smith, L. C. (2014). Toward global mapping of river discharge using satellite images and at-many-stations hydraulic geometry. *Proceedings of the National Academy of Sciences of the United States of America*, *111*(13), 4788–4791.

Godsey, S. E., & Kirchner, J. W. (2014). Dynamic, discontinuous stream networks: Hydrologically driven variations in active drainage density, flowing channels and stream order. *Hydrological Processes*, *28*(23), 5791–5803.

Goulsbra, C., Evans, M., & Lindsay, J. (2014). Temporary streams in a peatland catchment: Pattern, timing, and controls on stream network expansion and contraction. *Earth Surface Processes and Landforms*, *39*(6), 790–803.

Hannah, D. M., Demuth, S., van Lanen, H. A. J., Looser, U., Prudhomme, C., Rees, G., Stahl, K., & Tallaksen, L. M. (2011). Large-scale river flow archives: Importance, current status and future needs. *Hydrological Processes*, *25*(7), 1191–1200.

Heiner, B., Barfuss, S., & Johnson, M. (2011). Conditional assessment of flow measurement accuracy. *Journal of Irrigation and Drainage Engineering*, *137*(6), 367–374.

Hudson, L. N., Blagoderov, V., Heaton, A., Holtzhausen, P., Livermore, L., Price, B. W., van der Walt, S., & Smith, V. S. (2015). Inselect: Automating the digitization of natural history collections. *PLoS One*, *10*(11), 1–15.

HVZ-Baden-W rttemberg (2021). Hochwasservorhersagezentrale (hvz) baden-w rttemberg -pegel ebnet. https://hvz.baden-wuerttemberg.de/pegel.html?id=00389.

Jensen, C. K., McGuire, K. J., McLaughlin, D. L., & Scott, D. T. (2019). Quantifying spatiotemporal variation in headwater stream length using flow intermittency sensors. *Environmental Monitoring and Assessment*, *191*(4), 226.

Jensen, C. K., McGuire, K. J., & Prince, P. S. (2017). Headwater stream length dynamics across four physiographic provinces of the a ppalachian highlands. *Hydrological Processes*, *31*(19), 3350–3363.

Jensen, C. K., McGuire, K. J., Shao, Y., & AndrewDolloff, C. (2018). Modelingwet headwater streamnetworks across multiple flow conditions in the appalachian highlands. *Earth Surface Processes and Landforms*, *43*(13), 2762–2778.

Kalaitzakis, M., Cain, B., Carroll, S., Ambrosi, A., Whitehead, C., & Vitzilaios, N. (2021). Fiducial markers for pose estimation. *Journal of Intelligent & Robotic Systems*, *101*(4), 71.

Kaplan, N. H., Blume, T., & Weiler, M. (2020). Predicting probabilities of streamflow intermittency across a temperate mesoscale catchment. *Hydrology and Earth System Sciences*, *24*(11), 5453–5472.

Kaplan, N. H., Sohrt, E., Blume, T., & Weiler, M. (2019). *Time series of streamflow occurrence from 182 sites in ephemeral, intermittent and perennial streams in the attert catchment*.Luxembourg. V 2.0. GFZ Data Services.

Kotte, S., Rajesh Kumar, P., & Injeti, S. K. (2018). An efficient approach for optimal multilevel thresholding selection for gray scale images based on improved differential search algorithm. *Ain Shams Engineering Journal*, *9*(4), 1043–1067.

Kuo, L.-C., & Tai, C.-C. (2022). Robust image-based water-level estimation using single-camera monitoring. *IEEE Transactions on Instrumentation and Measurement*, *71*, 1–11.

Larson, P., & Runyan, C. (2009). *Evaluation of a capacitance water level recorder and calibration methods in an urban environment*. University of Maryland.

LAWA. (2018). *Leitfaden zur Hydrometrie des Bundes und der Länder - Pegelhandbuch*. Kulturbuch-Verlag GmbH.

Leduc, P., Ashmore, P., & Sjogren, D. (2018). Technical note: Stage and water width measurement of a mountain stream using a simple time-lapse camera. *Hydrology and Earth System Sciences*, *22*(1), 1–11.

Leigh, C., & Datry, T. (2017). Drying as a primary hydrological determinant of biodiversity in river systems: A broad-scale analysis. *Ecography*, *40*(4), 487–499.

Ljubičić, R., Strelnikova, D., Perks, M. T., Eltner, A., Peña-Haro, S., Pizarro, A., Dal Sasso, S. F., Scherling, U., Vuono, P., & Manfreda, S. (2021). A comparison of tools and techniques for stabilising unmanned aerial system (UAS) imagery for surface flow observations. *Hydrology and Earth System Sciences*, *25*(9), 5105–5132.

Lovill, S. M., Hahm, W. J., & Dietrich, W. E. (2018). Drainage from the critical zone: Lithologic controls on the persistence and spatial extent of wetted channels during the summer dry season. *Water Resources Research*, *54*(8), 5702–5726.

Ltd, D. S. (2012). Odyssey data logging software operating manual. http://odysseydatarecording.com/download/Odysse.

Ody Ltd. (2013). Odyssey capacitive water level logger. http://odysseydatarecording.com/download/OdysseyCapacitiveWaterLevelLogger2013.pdf.

Meerveld, H. J. I., Sauquet, E., Gallart, F., Sefton, C., Seibert, J., & Bishop, K. (2020). Aqua temporaria incognita. *Hydrological Processes*, *34*(26), 5704–5711.

Messager, M. L., Lehner, B., Cockburn, C., Lamouroux, N., Pella, H., Snelder, T., Tockner, K., Trautmann, T., Watt, C., & Datry, T. (2021). Global prevalence of non-perennial rivers and streams. *Nature*, *594*(7863), 391–397.

Olson, S. & Brouillette, M. (2006). A logistic regression equation for estimating the probability of a stream in Vermont having intermittent flow. https://pubs.usgs.gov/sir/2006/5217/

Otsu, N. (1979). A threshold selection method from gray-level histograms. *IEEE Transactions on Systems, Man, and Cybernetics*, *9*(1), 62–66.

Pandya, K. H., & Galiyawala, H. J. (2014). A survey on qr codes: In context of research and application. *International Journal of Emerging Technology and Advanced Engineering*, *4*(3), 258–262.

Pastor, A. V., Tzoraki, O., Bruno, D., Kaletová, T., Mendoza-Lera, C., Alamanos, A., Brummer, M., Datry, T., de Girolamo, A. M., Jakubínský, J., Logar, I., Loures, L., Ilhéu, M., Koundouri, P., Nunes, J., Quintas-Soriano, C., Sykes, T., Truchy, A., Tsani, S., & Jorda-Capdevila, D. (2022). Rethinking ecosystem service indicators for their application to intermittent rivers. *Ecological Indicators*, *137*, 108693.

Peirce, S., & Lindsay, J. (2015). Characterizing ephemeral streams in a southern Ontario watershed using electrical resistance sensors. *Hydrological Processes*, *29*(1), 103–111.

Perks, M. T., Dal Sasso, S. F., Hauet, A., Jamieson, E., Le Coz, J., Pearce, S., Peña-Haro, S., Pizarro, A., Strelnikova, D., Tauro, F., Bomhof, J., Grimaldi, S., Goulet, A., Hortobágyi, B., Jodeau, M., Käfer, S., Ljubičić, R., Maddock, I., Mayr, P., … Manfreda, S. (2020). Towards harmonisation of image velocimetry techniques for river surface velocity observations. *Earth System Science Data*, *12*(3), 1545–1559.

Piton, G., Recking, A., Le Coz, J., Bellot, H., Hauet, A., & Jodeau, M. (2018). Reconstructing depth–averaged open–channel flows using image velocimetry and photogrammetry. *Water Resources Research*, *54*(6), 4164–4179.

Roelens, J., Rosier, I., Dondeyne, S., van Orshoven, J., & Diels, J. (2018). Extracting drainage networks and their connectivity using lidar data. *Hydrological Processes*, *32*(8), 1026–1037.

Royem, A. A., Mui, C. K., Fuka, D. R., & Walter, M. T. (2012). Technical note: Proposing a low-tech, affordable, accurate stream stage monitoring system. *Transactions of the ASABE*, *55*(6), 2237–2242.

Sauter, T., Weitzenkamp, B., & Schneider, C. (2010). Spatio-temporal prediction of snow cover in the black forest mountain range using remote sensing and a recurrent neural network. *International Journal of Climatology*, *30*(15), 2330–2341.

Schneider, C. A., Rasband, W. S., & Eliceiri, K. W. (2012). Nih image to imagej: 25 years of image analysis. *Nature Methods*, *9*(7), 671–675.

Schoener, G. (2018). Time-lapse photography: Low-cost, low-tech alternative for monitoring flow depth. *Journal of Hydrologic Engineering*, *23*(2), 06017007.

Seibert, J., Strobl, B., Etter, S., Hummer, P., & van Meerveld, H. J. (2019). Virtual staff gauges for crowd-based stream level observations. *Frontiers in Earth Science*, *7*, 70.

Senatore, A., Micieli, M., Liotti, A., Durighetto, N., Mendicino, G., & Botter, G. (2021). Monitoring and modeling drainage network contraction and dry down in mediterranean headwater catchments. *Water Resources Research*, *57*(6), e2020WR028741.

Shaw, S. B. (2016). Investigating the linkage between streamflow recession rates and channel network contraction in a mesoscale catchment in New York state. *Hydrological Processes*, *30*(3), 479–492.

Shaw, S. B., Bonville, D. B., & Chandler, D. G. (2017). Combining observations of channel network contraction and spatial discharge variation to inform spatial controls on baseflow in birch creek, catskill mountains, USA. *Journal of Hydrology: Regional Studies*, *12*, 1–12.

Spence, C., & Mengistu, S. (2016). Deployment of an unmanned aerial system to assist in mapping an intermittent stream. *Hydrological Processes*, *30*(3), 493–500.

Stoll, S., & Weiler, M. (2010). Explicit simulations of stream networks to guide hydrological modelling in ungauged basins. *Hydrology and Earth System Sciences*, *14*(8), 1435–1448.

Strobl, B., Etter, S., van Meerveld, I., & Seibert, J. (2020). Accuracy of crowdsourced streamflow and stream level class estimates. *Hydrological Sciences Journal*, *65*(5), 823–841.

Uhlenbrook, S. (1999). Untersuchung und modellierung der abflussbildung in einem mesoskaligen einzugsgebiet. *Freiburger Schriften zur Hydrologie*, *10*(10), 201.

Uhlenbrook, S., Frey, M., Leibundgut, C., & Maloszewski, P. (2002). Hydrograph separations in a mesoscale mountainous basin at event and seasonal timescales. *Water Resources Research*, *38*(6), 31–1–31–14.

Uhlenbrook, S., Roser, S., & Tilch, N. (2004). Hydrological process representation at the meso-scale: The potential of a distributed, conceptual catchment model. *Journal of Hydrology*, *291*(3–4), 278–296.

van Loon, A. F. (2015). Hydrological drought explained. *WIREs Water*, *2*(4), 359–392.

Ward, A. S., Schmadel, N. M., & Wondzell, S. M. (2018). Simulation of dynamic expansion, contraction, and connectivity in a mountain stream network. *Advances inWater Resources*, *114*, 64–82.

Whiting, J. A., & Godsey, S. E. (2016). Discontinuous headwater stream networks with stable flowheads, salmon nriver basin, Idaho. *Hydrological Processes*, *30*(13), 2305–2316.

Wissmeier, L., & Uhlenbrook, S. (2007). Distributed, high-resolution modelling of 18o signals in a meso-scale catchment. *Journal of Hydrology*, *332*(3–4), 497–510.

Young, D. S., Hart, J. K., & Martinez, K. (2015). Image analysis techniques to estimate river discharge using time-lapse cameras in remote locations. *Computers & Geosciences*, *76*, 1–10.

Zanetti, F., Durighetto, N., Vingiani, F., & Botter, G. (2022). Analysing river network dynamics and active length - discharge relationship using water presence sensors. *Hydrology and Earth System Sciences Discussions*, *26*, 3497–3516.

Zhang, Z., Zhou, Y., Liu, H., & Gao, H. (2019). In-situ water level measurement using nir-imaging video camera. *Flow Measurement and Instrumentation*, *67*, 95–106.

Zimmer, M. A., Kaiser, K. E., Blaszczak, J. R., Zipper, S. C., Hammond, J. C., Fritz, K. M., Costigan, K. H., Hosen, J., Godsey, S. E., Allen, G. H., Kampf, S., Burrows, R. M., Krabbenhoft, C. A., Dodds, W., Hale, R., Olden, J. D., Shanafield, M., Del Vecchia, A. G., Ward, A. S., … Allen, D. C. (2020). Zero or not? Causes and consequences of zero-flow stream gage readings. *WIREs Water*, *7*(3), 1–25.

Zimmer, M. A., & McGlynn, B. L. (2017). Ephemeral and intermittent runoff generation processes in a low relief, highly weathered catchment. *Water Resources Research*, *53*(8), 7055–7077.

SUPPORTING INFORMATION

Additional supporting information can be found online in the Supporting Information section at the end of this article.

How to cite this article: Herzog, A., Stahl, K., Blauhut, V., & Weiler, M. (2022). Measuring zero water level in stream reaches: A comparison of an image-based versus a conventional method. *Hydrological Processes*, *36*(8), e14658. https://doi.org/10.1002/hyp.14658